J Appl Biol Chem (2023) 66:1, 1−6
https://doi.org/10.3839/jabc.2023.001

Online ISSN 2234-7941
Print ISSN 1976-0442

Article: Bioactive Materials

Bacterial neuraminidase inhibitory linarin from *Dendranthema zawadskii*

Ju Yeon Kim · Jae Yeon Park · Yun Gon Son · Kyu Lim Kim · Jeong Yoon Kim

Received: 14 December 2022 / Accepted: 6 January 2023 / Published Online: 13 January 2023

Abstract *Dendranthema zawadskii* is a one of the popular plants as native in South Korea. In this study, linarin was isolated and purified using silica-gel, Diaion, and Sephadex LH-20 from the aerial parts of *D. zawadskii*. The chemical structure was completely identified through spectroscopic data including 1D, 2D nucleic magnetic resonance, and HRFABMS. Furthermore, linarin inhibited the bacterial neuraminidase (BNA) activity with 13.5 μM of IC_{50} dose-dependently. Through the enzyme kinetic experiments, linarin as BNA inhibitor exhibited a typical noncompetitive inhibition mode which K_m was contestant and V_{max} decreased as the concentration of the inhibitor increased. It was further identified that the inhibition constant was 16.0 μM. Linarin was the most abundance metabolite in the aerial part of *D. zawadskii* extract by UHPLC-TOF/MS analysis. Therefore, *D. zawadskii* and its main component are expected that it can be effectively used for the infection and inflammation caused by bacteria.

Keywords Anti-inflammation · Bacterial neuraminidase · *Dendranthema zawadskii* · Linarin · Noncompetitive inhibitor

Introduction

Bacterial infection in living organism is closely related to inflammation and immunity [1]. Specifically, the infected bacteria through wounds promote the secretion of cytokines from macrophages, and these become the main cause of the inflammatory response [2,3]. Sometimes, bacteria in the inflamed site forms its cluster called as biofilms, which cause various biological problems such as sepsis, nerve damage, and delayed wound healing [4-6]. Bacterial neuraminidase (EC 3.2.1.18, BNA) is related with bacteria quorum sensing to produce the biofilm by cell-cell signaling [7,8]. BNA also known as acyl-neuraminyl hydrolase cleaves terminal α-ketosidic linkage between *N*-acetylneuraminic acid and the adjacent sugar moieties such as oligosaccharides, polysaccharides, mucopolysaccharides, glycoproteins, and glycolipids [9]. Through these processes, the fragmented sialic acid enables entry of pathogens into the host to cause inflammation [10]. It can be a clue to control of biofilm formation and anti-inflammation effects by inhibition the activity of BNA. Based on this hypothesis, we tried to investigate the BNA inhibitory activity of the main metabolite from *D. zawadskii* to confirm possibility as an anti-inflammatory nutraceutical.

Dendranthema zawadskii is a perennial plant of the Asteraceae family and is native to Southern Asia such as Japan, China, and South Korea [11,12]. It has been known as an herbal medicine effective for indigestion, menstrual irregularity, and stomach since ancient times [13]. According to previous reports, flavonoids and caffeoyl quinic acid derivatives are known as bioactive phytochemicals from *D. zawadskii* [14,15]. In particular, linarin belonging to a glycosylated flavone is overwhelmingly present as the main compound in *D. zawadskii* extract. It has been well reported that linarin has anti-Alzheimer's, anti-viral, anti-bacterial, and anti-proliferation effects [16,17]. Along with these biological activities, it also has anti-inflammation by lowering virous factors such as NO, TNF-α, IL-6, and PGE2 [18]. Nevertheless, there has been no report regarding the ani-inflammatory effect caused by bacterial infection by inhibiting BNA activity.

In this study, linarin was isolated and purified using chromatographic experiments from the aerial part of *D. zawadskii*. The structural identification was completed with spectroscopic data. In addition, the anti-inflammatory activity of linarin was investigated as an inhibitory potential against BNA. The natural abundance of linarin was confirmed by using LC-Q-TOF/MS from *D. zawadskii*

Jeong Yoon Kim (✉)
E-mail: jykim21@gnu.ac.kr

Department of Pharmaceutical Engineering, IALS, Gyeongsang National University, Jinju 52725, Republic of Korea

extract. Therefore, we tried to develop new nutraceutical values of *D. zawadskii* by applying BNA inhibitory activity.

Materials and Methods

Plant and chemicals

Dried aerial parts of *D. zawadskii* was purchased from local market at Sojeong-myeon, Sejong-si, South Korea. The local market guaranteed that the plant was collected and packaged in June 2021 with the permit registration number (2015-0365486). Silica-gel (230-400 mesh, Merck, Darmstadt, Germany), Diaion-HP20 (Sigma Aldrich, St. Louis, Missouri, USA), and Sephadex LH-20 (GE Healthcare, Chicago, Il, USA) were used for isolation and identification of linarin. Methanol, chloroform, and acetone was bought from Daejeong chemical & metals (Siheung-si, Gyeonggi-do, South Korea). For the enzyme inhibition assay, neuraminidase from *Clostridium perfringens*, 2'-(4-methylumbelliferyl)-α-D-*N*-acetylneuraminic acid sodium salt hydrate, dimethyl sulfoxide, and apigenin was purchased from Sigma Aldrich. Acetonitrile and water for HPLC experiments was used as analytical solvents from Honeywell (Charlotte, NC, USA).

Apparatus

The chemical structure of isolate compound was identified using nucleic magnetic resonance (NMR) AM 500 (Bruker, Karlsruhe, Germany) resulting in ^{1}H, ^{13}C-NMR, HMBC, and HMQC. Furthermore, the chemical formula was obtained from HRFABMS (JMS-700, JEOL, Tokyo, Japan). The BNA inhibitory activity was conducted using iD3 spectrophotometer (Molecular devices, Sunnyvale, CA, USA) having fluorescence intensity measuring system by time with thermostat. Natural abundance of *D. zawadskii* was analyzed by using NEXERA UHPLC (Shimadzu, Kyoto, Japan) connected with TOF/MS (X500R, Sciex, WA, USA).

Isolation and identification of linarin from *D. zawadskii*

The aerial parts of *D. zawadskii* (100 g) extracted with methanol (1 L×3) for 3 h using sonication. The plant solution was evaporated to yield crude extract (12 g). To remove the chlorophyll, the extract was injected on open column packed with Diaion HP-20 mixed in 80% methanol, then target metabolites and chlorophylls layer were completely gain from eluting with methanol and acetone, respectively. Among them, the methanol layer (8 g) was fractionated using silica-gel open column (30×500 mm, 150 g) eluting with solution of combination between chloroform and methanol (*v*/*v*, 50:1 → 1:1) to afford five fractions (Fr. 1~Fr. 5). The major component enriched Fr. 3 (1.6 g) was purified using Sephadex LH-20 eluting with 80% methanol to give single compound (320 mg). The structure of the isolated compound was found to be linarin by NMR and HRFABMS, comparing with the literature [19]. The detailed spectroscopic data are as shown in Table 1.

Table 1 ^{1}H and ^{13}C NMR spectroscopic data of linarin (DMSO-d_6)

No	δ_H, multi (*J*, Hz)	δ_C
2		164.43
3	6.95 (s)	104.29
4		182.51
4a		105.95
5		161.63
6	6.46 (d, *J* = 2.0 Hz)	100.14
7		163.44
8	6.80 (d, *J* = 1.9 Hz)	95.27
8a		157.46
1'		123.15
2'	8.05 (d, *J* = 8.8 Hz)	128.94
3'	7.15 (d, *J* = 8.9 Hz)	115.19
4'		162.91
5'	7.15 (d, *J* = 8.9 Hz)	115.19
6'	8.05 (d, *J* = 8.8 Hz)	128.94
2"	5.07 (d, *J* = 7.3 Hz)	100.42
3"	3.29, m	73.55
4"	3.30	76.74
5"	3.68	70.81
6"	3.62	76.14
7"	3.44, 3.88	66.58
8"	4.56 (s)	101.01
9"	3.48	71.24
10"	3.16	70.04
11"	3.17	72.46
12"	3.42	68.87
4'-OCH_3	3.87 (s)	56.05
12"-CH_3	1.09 (d, *J* = 6.2 Hz)	18.29
5-OH	12.91 (s)	

Bacterial neuraminidase inhibitory activity

Neuraminidase from *Clostridium perfringens* (*C. welchii*, EC 3.2.1.18) was hydrolyzed 4-methylumbelliferyl-N-acetyl-α-D-neuraminic acid (4-MUNANA) by fluorogenic acid [20]. The products of umbelliferone from 4-MUNANA is one of coumarin derivatives, it can act at 365 nm of excitation wavelength and detect at 450 nm of emission wavelength. The BNA activity was investigated in reaction solution combined with 160 μL of 50 mM sodium acetate buffer, 10 μL of linarin (0, 3.13, 6.25, 12.5, 25, and 50 μM), 20 μL of 4-MUNANA (100 μM), and 10 μL of BNA (0.02 unit/mL). The mixture was placed in black/flat bottom 96 well plant and measured for 10 min at 37 °C. The inhibitory potencies were determined following equation: fluorescence intensity of [(linarin – vehicle)/vehicle]×100 (%)

2.4. Enzyme kinetic experiments

After confirming the inhibitory activity, the enzyme inhibitory mode was investigated on BNA. The reversibility of linarin was determined by administering three concentrations of BNA (0.01, 0.02, and 0.04 unit/mL) with inhibitor. In addition, the kinetic

mode and inhibition constant were evaluated from Lineweaver-Burk and Dixon plots, respectively. First, three concentrations of substrate (×0.5, ×1, and ×2 K_m) and inhibitor (×0.5, ×1, and ×2 IC_{50}) in buffer were measured with BNA (0.2 unit/mL). The reaction solution was measured using fluorometric method at 365 and 450 nm of excitation and emission wavelength on 96 well immuno plate.

2.5. UHPLC-Q-TOF/MS condition

UHPLC performed by the gradient procedure with increasing solvent portion (*v*/*v*) of acetonitrile in water reached from 0% to 100% within 60 min. The flow rate was 0.3 mL/min and the column was Poroshell 120 EC-C18 (2.1×100 mm, 2.7 μm, Agilent technologies, Santa Clara, CA, USA). For Q-TOF/MS analysis, the ionization was set the ranges from 100 to 10000 Da in the negative ion mode. The ion source (TurboSpray) condition were 5500 V of ion spray voltage and 550 °C of source temperature. The nitrogen gas (GS1 and GS2) and curtain gas flow were 50 psi and 30 psi, respectively. A collision energy from 10 to 50 eV was obtained with an accumulation time of 0.1 s with controlled Q1 windows. Declustering potential was optimized at 50 V. Data processing software was SCIEX OS V1.5 for mass spectra.

Statistical analysis

All experiments were performed more than three times. The plot derived for BNA inhibition and the calculation of statistical result values carried out using Sigma plot ver. 10.0.

Results and Discussions

Structural identification of linarin

The main compound from the methanol extract of *D. zawadskii* was isolated using silica-gel and Sephadex LH-20. The isolated one was identified by linarin as a glycosylated flavone as shown in Fig. 1. Spectroscopic data of the isolated compound agreed with previous reports [19].

Linarin was isolated as a light-yellow powder with molecular formula $C_{28}H_{32}O_{14}$ established by the [M]+ ion at 593.1852 (calcd 593.1870) in the HRFABMS. The presence of 8 quaternary carbons, 17 methine carbons (7 sp^2 and 10 sp^3), 1 methylene carbon, and 2 methyl carbons was confirmed by DEPT analysis. The isolated compound was estimated to consist of 5 rings and 8 double carbons from 13 of unsaturated degrees by ^{1}H, ^{13}C-NMR, and HRFABMS. In the ^{1}H-NMR spectrum, a flavone skeleton was elucidated with a *meta*-coupling between H-6 (δ_H 6.46, d, J=2.0 Hz) and H-8 (δ_H 6.80, d, J=1.9 Hz) in A-ring, and the representative peak of H-3 at δ_H 6.95. The methoxy group in the B-ring was deduced from a coupling between H-2'/6' (δ_H 8.05, d, J=8.8 Hz, 2H) and H-3'/5' (δ_H 7.15, d, J=8.9 Hz, 2H), and the correlation of methoxy proton (δ_H 3.87, s, 3H) to C-4' (δ_C 162.91) by HMBC. The rutinoside motif at C-7 was confirmed by strong correlations with an anomeric proton of rhamnose (δ_H 4.56) to methylene carbon (δ_C 66.58) and an anomeric proton of glucose (δ_H 5.07) to C-7 (δ_C 163.45) by HMBC. Thus, the compound was determined to 5-hydroxy-2-(4-methoxyphenyl)-7-[(2S,3R,4S,5S,6R)-3,4,5-trihydroxy-6-[[(2R,3R,4R,5R,6S)-3,4,5-trihydroxy-6-methyloxan-2-yl]oxymethyl]oxan-2-yl]oxychromen-4-one, called as linarin.

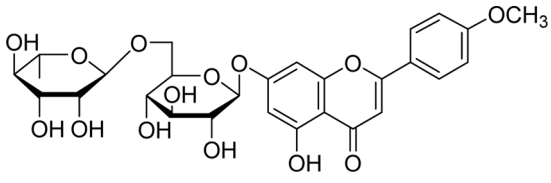

Fig. 1 Chemical structure of linarin from the aerial part of *D. zawadskii*

Bacterial neuraminidase inhibition assay

As shown in Fig. 2 and Table 2, linarin was investigated for its anti-inflammation effects by confirmation of the dose-dependence, reversibility, and enzyme kinetics against BNA. The inhibitory capacity against BNA was derived from the target enzyme and the different concentrations of tested samples. The methanol extract of *D. zawadskii* exhibited 80% BNA inhibition at 150 μg/mL. The main component of *D. zawadskii* extract, linarin, was inhibited BNA activity in dose-dependent manners with 13.5 μM of IC_{50} value (Fig. 2A). It was 2-fold more effective than apigenin (IC_{50} =34.6 μM), which was a basic skeleton of linarin used as a positive control. Therefore, it is found that the rutinoside motif at A-ring of linarin had mainly affected on BNA inhibitory effects.

In kinetic analysis, linarin was a reversible inhibitor against BNA, because the lines of inhibitor (6.25, 12.5, and 25.0 μM) passed through the origin of the plots at different concentrations of BNA (0.01, 0.02, and 0.04 unit/mL) in Fig. 2B. As shown in Fig. 3C, the inhibition modes of linarin was displayed by plotted from Lineweaver-Burk. At the fixed concentration of BNA, it showed the assembled straight lines of linarin on the *x*-axis related to the different concentrations of substrates. Therefore, the plots showed V_{max} values were decreased, but K_m values were constant as the concentration of the inhibitor increased. The inhibition constant (K_i) came from the point of successive lines of the substrate by Dixon plots (Fig. 2D). Thus, linarin was identified as a noncompetitive inhibitor with 16.0 μM of K_i value against BNA. It exhibited inhibition modes by binding to enzyme-substrate complex rather than to the active site of BNA.

UHPLC-Q-TOF/MS analysis of *D. zawadskii* extract

Figure 3 showed the natural abundance in the methanol extract of *D. zawadskii* using UHPLC-ESI-TOF/MS. In the chromatogram at 254 nm, the area of each peaks in the methanol extract of *D. zawadskii* was observed by automatically calculation from software SCIEX OS (Fig. 3 and Table 3). In the chromatogram, the most abundant one is peak 4 at 18.804 min, which was

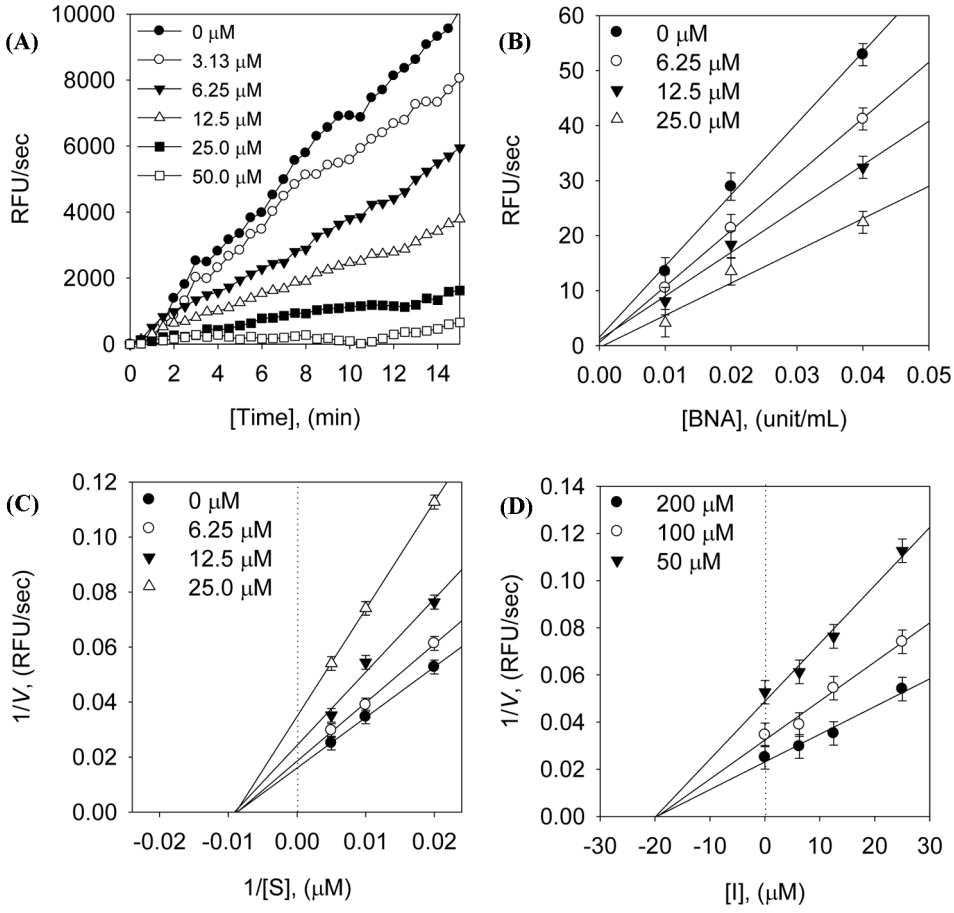

Fig. 2 Effects of BNA inhibition of linarin. (A) Fluorescence intensity of different concentrations of linarin (0, 3.13, 6.25, 12.5, 25, and 50 μM). (B) Reversibility, (C) Lineweaver-Burk plots, and (D) Dixion plots of linarin against BNA

significantly higher than peaks 1-3. The four major peaks (peaks 1-4) were assigned from the individual MS grams at the negative ion modes. Peak 1 (t_R =6.754 min, Fig. 3B) was identified as chlorogenic acid, because it had reasonable error value with −5.08 ppm by comparing between observed (*m/z* 355.1011) and calculated ion peaks (*m/z* 355.1029). Peak 2 (t_R =14.2 min, *m/z* 517.1324, Fig. 3C) and 3 (t_R =15.0 min, *m/z* 517.1326, Fig. 3D) had detected ion peaks at and *m/z* 517, which also had fragment ion at *m/z* 163 by cleaved bonds from dicaffeic acid and quinic acid. Thus, the peak 2 and 3 were identified as 3,5-dicaffeoylquinic acid and 3,4-dicaffeoulquinic acid according with previous reports. Peak 4 (t_R =18.7 min, Fig. 3E) had molecular ion peak at *m/z* 593.1838 and calculated ion peak at *m/z* 517.1870. Based on the results, the peak 4 was identified as linarin. Based on the results, it was also confirmed that linarin occupied more than 60% in the extract. Thus, *D. zawadskii* can expected the possibility of developing nutraceuticals to improve inflammation caused by bacterial infection because of containing BNA inhibitory linarin.

Table 2 BNA inhibitory effects of linarin from *D. zawadskii*

Compounds	IC_{50}[a] (μM)	Kinetic modes	K_i[b] (μM)
Linarin	13.5±0.5	Noncompetitive	16.0
Apigenin[c]	34.6±0.7	NT[d]	NT

[a]IC_{50} is the inhibitor concentration of inhibition rate at 50% to BNA activity
[b]K_i is the inhibition constant between enzyme and inhibitor
[c]Apigenin is used as the positive control
[d]NT is not tested

Table 3 Identification of metabolites from the aerial part of *D. zawadskii* by UHPLC-Q-TOF/MS analysis

Peaks	Retention time (min)	Detected ion (*m/z*)	Calculated ion (*m/z*)	Error (ppm)	Identification
1	6.7	355.1011	355.1029	-5.08	Chlorogenic acid
2	14.2	517.1324	517.1346	-4.25	3,5-Dicaffeoylquinic acid
3	15.0	517.1326	517.1346	-3.87	3,4-Dicaffeoylquinic acid
4	18.7	593.1838	593.1870	-5.40	Linarin

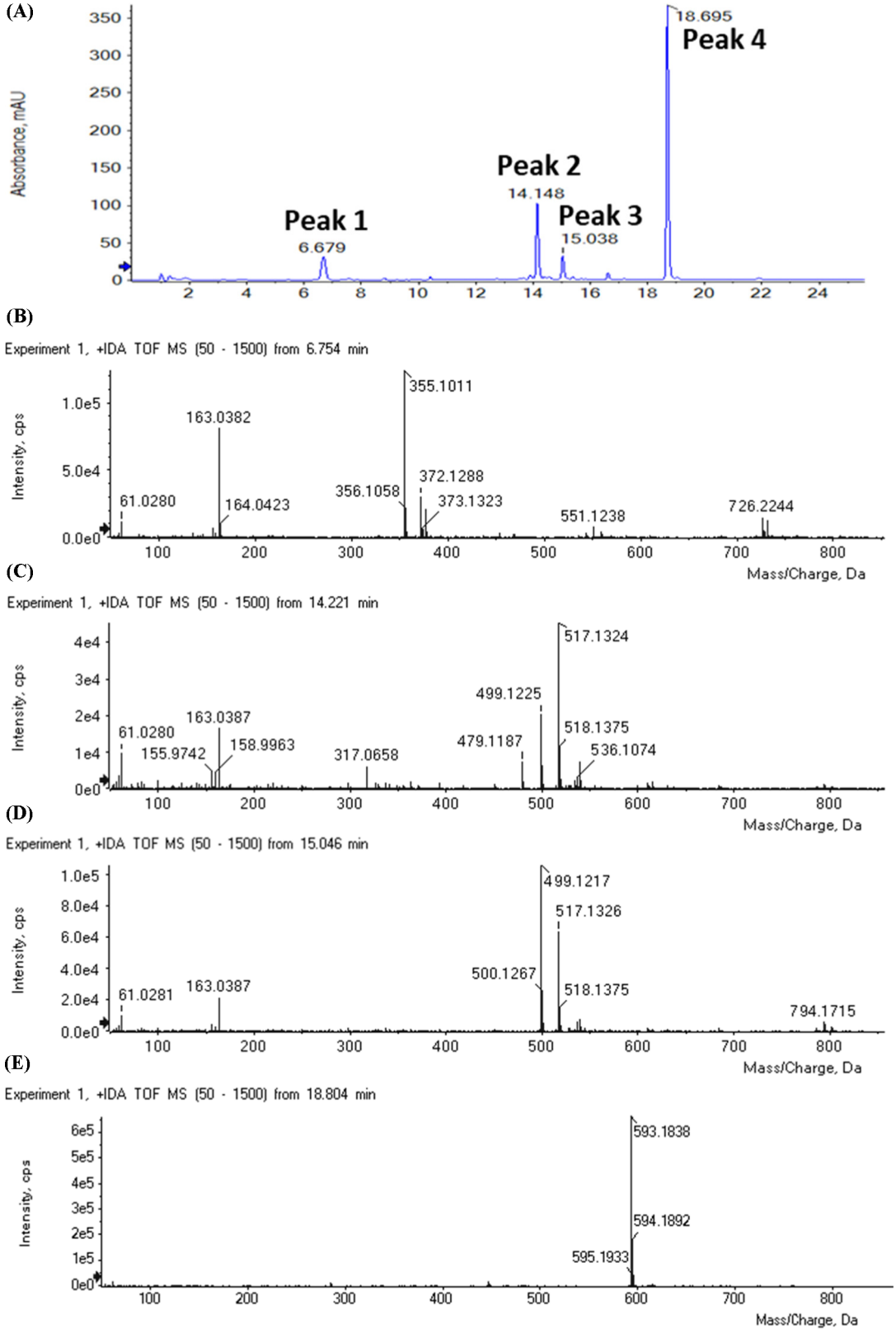

Fig. 3 UHPLC-Q-TOF/MS analysis of the methanol extract of *D. zawadskii*. (A) DAD chromatogram of *D. zawadskii* extract at 254 nm. (B-E) Mass gram of peaks 1-4 by TOF/MS

Acknowledgment This work was supported by the National Research Foundation of Korea (NRF) grant funded by the Korea government (MSIT), 2021R1A5A8029490 and 2022R1F1A1063786.

References

1. Belkaid Y, Hand TW (2014) Role of the Microbiota in Immunity and inflammation. Cell 157: 121. doi: 10.1016/J.CELL.2014.03.011
2. Chen L, Deng H, Cui H, Fang J, Zuo Z, Deng J, Li Y, Wang X, Zhao L (2018) Inflammatory responses and inflammation-associated diseases in organs. Oncotarget 9: 7204. doi: 10.18632/ONCOTARGET.23208
3. Krzyszczyk P, Schloss R, Palmer A, Berthiaume F (2018) The role of macrophages in acute and chronic wound healing and interventions to promote pro-wound healing phenotypes. Front Physiol 9: 419. doi: 10.3389/FPHYS.2018.00419/BIBTEX
4. Snowden JN, Beaver M, Smeltzer MS, Kielian T (2012) Biofilm-Infected Intracerebroventricular Shunts Elicit Inflammation within the Central Nervous System. Infect Immun 80: 3206. doi: 10.1128/IAI.00645-12
5. Percival SL, McCarty SM, Lipsky B (2015) Biofilms and Wounds: An Overview of the Evidence. Adv Wound Care 4: 373. doi: 10.1089/WOUND.2014.0557
6. Minasyan H (2019) Sepsis: mechanisms of bacterial injury to the patient. Scand J Trauma, Resusc Emerg Med 2019 271 27: 1–22. doi: 10.1186/S13049-019-0596-4
7. Soong G, Muir A, Gomez MI, Waks J, Reddy B, Planet P, Singh PK, Kanetko Y, Wolfgang MC, Hsiao YS, Tong L, Prince A (2006) Bacterial neuraminidase facilitates mucosal infection by participating in biofilm production. J Clin Invest 116: 2297–2305. doi: 10.1172/JCI27920
8. Bowles WHD, Gloster TM (2021) Sialidase and Sialyltransferase Inhibitors: Targeting Pathogenicity and Disease. Front Mol Biosci 8: 705. doi: 10.3389/FMOLB.2021.705133/BIBTEX
9. Schauer R, Kamerling JP (2018) Exploration of the Sialic Acid World. Adv Carbohydr Chem Biochem 75: 1. doi: 10.1016/BS.ACCB.2018.09.001
10. Jennings MP, Day CJ, Atack JM (2022) How bacteria utilize sialic acid during interactions with the host: snip, snatch, dispatch, match and attach. Microbiology 168: 1157. doi: 10.1099/mic.0.001157
11. Hao DC, Song Y, Xiao P, Zhong Y, Wu P, Xu L (2022) The genus Chrysanthemum: Phylogeny, biodiversity, phytometabolites, and chemodiversity. Front Plant Sci 13: 2793. doi: 10.3389/FPLS.2022.973197/BIBTEX
12. Kang JH, Kim JS (2020) New diploid populations of *Chrysanthemum indicum* L. (Asteraceae) from Korea. Korean J Plant Taxon 50: 17–21. doi: 10.11110/KJPT.2020.50.1.17
13. Kim AR, Kim HS, Kim DK, Lee JH, Yoo YH, Kim JY, Park SK, Nam ST, Kim HW, Park YH, Lee D, Lee MB, Kim YM, Choi WS (2016) The Extract of Chrysanthemum zawadskii var. latilobum Ameliorates Collagen-Induced Arthritis in Mice. Evidence-based Complement Altern Med 2016. doi: 10.1155/2016/3915013
14. Lai JP, Lim YH, Su J, Shen HM, Ong CN (2007) Identification and characterization of major flavonoids and caffeoylquinic acids in three Compositae plants by LC/DAD-APCI/MS. J Chromatogr B 848: 215–225. doi: 10.1016/j.jchromb.2006.10.028
15. Clifford MN, Wu W, Kirkpatrick J, Kuhnert N (2007) Profiling the chlorogenic acids and other caffeic acid derivatives of herbalChrysanthemum by LC-MS. J Agric Food Chem 55: 929–936. doi: 10.1021/jf062314x
16. Fan P, Hay AE, Marston A, Hostettmann K (2008) Acetylcholinesterase-Inhibitory Activity of Linarin from Buddleja davidii, Structure-Activity Relationships of Related Flavonoids, and Chemical Investigation of Buddleja nitida. 46: 596–601. doi: 10.1080/13880200802179592
17. Mottaghipisheh J, Taghrir H, Dehsheikh AB, Zomorodian K, Irajie C, Sourestani MM, Iraji A (2021) Linarin, a glycosylated flavonoid, with potential therapeutic attributes: A comprehensive review. Pharmaceuticals 14: 1104. doi: 10.3390/PH14111104/S1
18. Han S, Sung KH, Yim D, Lee S, Lee CK, Ha NJ, Kim K (2002) The Effect of linarin on LPS-induced cytokine production and nitric oxide inhibition in murine macrophages cell line RAW264.7. Arch Pharm Res 25: 170–177. doi: 10.1007/bf02976559
19. Erenler R, Telci İ, Elmastaş M, Aksit H, Gül F, Rıza TÜFEKÇİ A, Demirtaş İ, Kayir Ö (2018) Quantification of flavonoids isolated from Mentha spicata in selected clones of Turkish mint landraces. 42: 1695–1705. doi: 10.3906/kim-1712-3
20. Hurt AC (2007) Fluorometric Neuraminidase Inhibition Assay. Stand Oper Proced WHO, Geneva